C.-S. Wang

M. M. Yovanovich
Fellow ASME

J. R. Culham
Mem. ASME

Microelectronics Heat Transfer Laboratory,
Department of Mechanical Engineering,
University of Waterloo,
Waterloo, Ontario, Canada N2L 3G1

Modeling Natural Convection From Horizontal Isothermal Annular Heat Sinks

A study is presented for laminar natural convection heat transfer from isothermal, vertical disks with horizontal support cylinders, as found in annular-fin heat sinks. A distinction is made between the external and internal surfaces of the heat sink, and, hence, the heat transfer mechanisms which dominate in each of these surfaces can be more easily applied. A boundary layer solution for laminar natural convection, a fully developed flow solution, and a diffusive limit are successfully applied to this complex geometry to form the present model. The model shows good agreement with present experimental data and previous correlations.

Introduction

Annular-fin heat sinks are used for cooling components in electronic systems and other equipment. A schematic of the annular-fin heat sink used in this study is shown in Fig. 1 in the horizontal orientation, where the gravity force is parallel to the annular fins. The heat sink consists of N_f identical fins with a centrally located circular support cylinder. Each fin has a fin thickness, t, an outer diameter, D, and an inner diameter, d. Adjacent fins are separated by a distance, b, and the overall length of the heat sink is L. The surface of the heat sink was assumed isothermal in this study. Nonisothermal surfaces are also discussed in the Application Related Issues section.

The spacing b is used as the characteristic length (Elenbaas, 1942; Edwards and Chaddock, 1963; Jones and Nwizu, 1969; Tsubouchi and Masuda, 1970). The Nusselt number is defined as

$$\mathrm{Nu} = \frac{Q}{A\Delta T}\frac{b}{k}, \tag{1}$$

and the Elenbaas Rayleigh number is (Elenbaas, 1942; Edwards and Chaddock, 1963; Jones and Nwizu, 1969; Tsubouchi and Masuda, 1970)

$$\mathrm{Ra} = \frac{g\beta\Delta T b^3}{\alpha\nu}\frac{b}{D}, \tag{2}$$

where ΔT is the temperature difference between the heat sink surface and the ambient air.

As shown in Fig. 1, a heat sink surface consists of four types of component surfaces, i.e., lateral fin surfaces, support cylinder surfaces, fin rim surfaces and end surfaces. The combination of all lateral fin surfaces and support cylinder surfaces is referred to as the inner surface, with the area A_{IN}; the fin rim surfaces and the end surfaces are considered as the outer surface, with the area A_{OUT}. The sum of A_{IN} and A_{OUT} is the total heat sink surface area A_{HS}. The heat transfer mechanism of the inner surface is fundamentally different from that of the outer surface. The inner surface may experience three regimes of heat transfer: thin boundary layer convection at high Ra, fully developed flow at low Ra and a transitional regime. While over the outer surface of the heat sink, there is only one mode of heat transfer for the entire range of Ra, i.e., external natural convection. At low Ra, the heat flux of the inner surface is much smaller than that of the outer surface, because the inner surface is in a fully developed regime, while the outer surface is associated with boundary layer heat transfer. Therefore at low Ra, the surface area ratio A_{OUT}/A_{HS} is an important factor which determines the magnitude of the heat sink Nusselt number. If A_{OUT}/A_{HS} is large, the heat sink Nusselt number will be large at low Ra.

Most previous models for calculating heat transfer from annular heat sinks do not recognize the fundamental difference in heat transfer over the inner and outer surfaces and therefore models based on this premise do not provide an accurate measure of the thermal behavior. Several correlations for natural convection heat transfer from annular-fin heat sinks can be found in the open literature. Edwards and Chaddock (1963) and Jones and Nwizu (1969) did not consider heat transfer from the inner and outer surfaces separately. As a result, their correlations can not be used for heat sinks with different area ratios of A_{OUT}/A_{HS} from that of their test heat sinks. For example, heat sinks used in electronic systems usually have only a few fins, and the end surface is a large portion of the total surface. The area ratio (A_{OUT}/A_{HS}) of these heat sinks are much larger than that of the test heat sinks of Edwards and Chaddock (1963) and Jones and Nwizu (1969), whose test heat sinks had 40 to 70 fins based on the same parameters t/D and b/D.

Tsubouchi and Masuda (1970) considered the inner and outer surfaces separately. They gave two correlations for the inner surface and the fin rim surface, respectively. But they did not consider the end surface cooling. They eliminated the heat transfer from the end surfaces in their experiments through the use of end guard sections. As a result their correlations are not suitable for heat sinks used in electronic systems either, where the end surface cooling plays a significant role in the total heat transfer.

The objective of this study is to treat the inner and the outer surfaces separately and establish a general model which accounts for the effects of all surfaces of the heat sink, including the ends and the fin rims. The model will be compared to previous correlations and new experimental data.

External Natural Convection Solutions

Yovanovich (1987b, c) and Lee et al. (1991) used a characteristic length based on the surface area, $\sqrt{A}$, to recast the existing boundary layer solutions for laminar natural convection (Acrivos, 1960; Stewart, 1971; Raithby and Hollands, 1975, 1978) and obtained a new expression of the solutions for isothermal, three dimensional bodies. When combined with the diffusive limit, the expression gives the total heat transfer as

Contributed by the Electrical and Electronic Packaging Division for publication in the JOURNAL OF ELECTRONIC PACKAGING. Manuscript received by the EEPD September 15, 1997; revision received July 10, 1998. Associate Technical Editor: R. Wirtz.

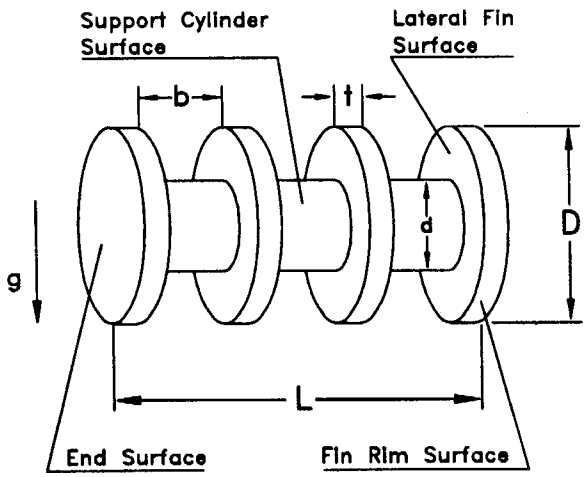

Fig. 1 Dimensions and surfaces of heat sink

$$\mathrm{Nu}_{\sqrt{A}} = \mathrm{Nu}^0_{\sqrt{A}} + F(\mathrm{Pr})G_{\sqrt{A}}\,\mathrm{Ra}^{1/4}_{\sqrt{A}}. \quad (3)$$

The first term of the equation, $\mathrm{Nu}^0_{\sqrt{A}}$, is the diffusive limit of the body, which accounts for the correction for the curvature effect of the boundary layers. The second term of the equation, $F(\mathrm{Pr})G_{\sqrt{A}}\mathrm{Ra}^{1/4}_{\sqrt{A}}$, is the boundary layer solution for the total surface, where $F(\mathrm{Pr})$ is the approximate "universal" Prandtl number function (Churchill and Churchill, 1975), defined as

$$F(\mathrm{Pr}) = 0.670/[1 + (0.5/\mathrm{Pr})^{9/16}]^{4/9}, \quad (4)$$

and $G_{\sqrt{A}}$ is the body-gravity function for two-dimensional or axisymmetric surfaces, which is (Yovanovich, 1987b, c)

$$G_{\sqrt{A}} = \left[\frac{1}{A}\int\int_A \left(\frac{P(\theta)\sin\theta}{\sqrt{A}}\right)^{1/3} dA\right]^{3/4}, \quad (5)$$

where A is the total area of the surface considered, $P(\theta)$ is the local perimeter of the axisymmetric body, and θ is the angle between the outward normal and the gravity vector.

The overall body-gravity function for N component surfaces connected in parallel with respect to the flow stream can be obtained by (Lee et al., 1991)

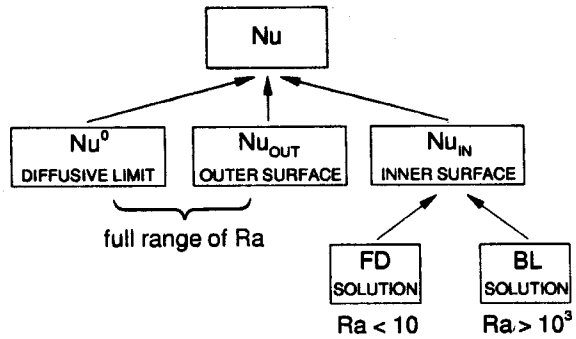

Fig. 2 Model composition

$$G_{\sqrt{A}} = \sum_{i=1}^{N} G_{\sqrt{A_i}}\,(A_i/A)^{7/8}, \quad (6)$$

where A_i refers to the component surface areas and A is the total surface area for the N component surfaces, which is given by $A = \sum_{i=1}^{N} A_i$.

The overall body-gravity function for component surfaces connected in series with respect to the flow stream can be obtained from (Lee et al., 1991)

$$G_{\sqrt{A}} = \left[\sum_{i=1}^{N} G^{4/3}_{\sqrt{A_i}}\,(A_i/A)^{7/6}\right]^{3/4}. \quad (7)$$

Model Development

Figure 2 gives a map of the various model components that will be considered in developing the present model. In Fig. 2, Nu is the Nusselt number for the heat sink; Nu^0 is the contribution by the diffusive limit; Nu_{OUT} is the contribution by the convection of the outer surface; and Nu_{IN} is the contribution by the convection of the inner surface, which is obtained through blending the fully developed flow solution and the boundary layer solution.

Based on the definitions of the Nusselt number, Eq. (1), and the Elenbaas Rayleigh number, Eq. (2), the natural convection solution Eq. (3) can be expressed as

Nomenclature

A = surface area, m^2
A_{CC} = surface area of circumscribed cylinder, $\equiv \pi D^2/2 + \pi DL$, m^2
A_{CS} = surface area of channel control surface, $\equiv \pi Db$, m^2
A_{CL} = surface area of a single channel, $\equiv \pi(D^2 - d^2)/2 + \pi db$, m^2
A_{IN} = inner surface area, $\equiv (N_f - 1)A_{CL}$, m^2
A_{OUT} = outer surface area, $\equiv \pi D^2/2 + N_f \pi Dt$, m^2
A_{HS} = total surface area of heat sink, $\equiv A_{IN} + A_{OUT}$, m^2
b = spacing between adjacent fins, m
D = fin outer diameter, m
d = diameter of support cylinder, m
$G_{\sqrt{A}}$ = body-gravity function, Eq. (5)
g = gravitational acceleration, m/s^2
k = thermal conductivity, W/mK
L = length of heat sink, $\equiv N_f(t + b) - b$, m
N_f = total number of fins
Nu^0 = diffusive limit Nusselt number as $\mathrm{Ra}_D \to 0$
$\mathrm{Nu}_{\sqrt{A}}$ = Nusselt number with $\sqrt{A}$ as the characteristic length, $\equiv Q\sqrt{A}/A\Delta Tk$
Nu = Nusselt number with b as the characteristic length, $\equiv Qb/A\Delta Tk$
n = Churchill-Usagi fit parameter
Q = heat flow rate by convection, W
$\mathrm{Ra}_{\sqrt{A}}$ = Rayleigh number with $\sqrt{A}$ as the characteristic length, $\equiv g\beta\Delta T(\sqrt{A})^3/\nu\alpha$
Ra = Elenbaas Rayleigh number, $\equiv g\beta\Delta Tb^4/\nu\alpha D$
Ra_D = Rayleigh number with D as the characteristic length, $\equiv g\beta\Delta TD^3/\nu\alpha$
T_S = surface temperature of heat sink, K
T_∞ = temperature of ambient air, K
t = fin thickness, m
ΔT = temperature difference, $\equiv T_S - T_\infty$, K
α = thermal diffusivity of air, m^2/s
β = volumetric coefficient of thermal expansion, 1/K
ν = kinematic viscosity, m^2/s

Subscripts

cf = channel flow, based on A_{CL}
cs = channel control surface, based on A_{CL}
bl = boundary layer flow of inner surface
fd = fully developed flow of inner surface
IN = inner surface contribution, based on A_{HS}
OUT = outer surface contribution, based on A_{HS}

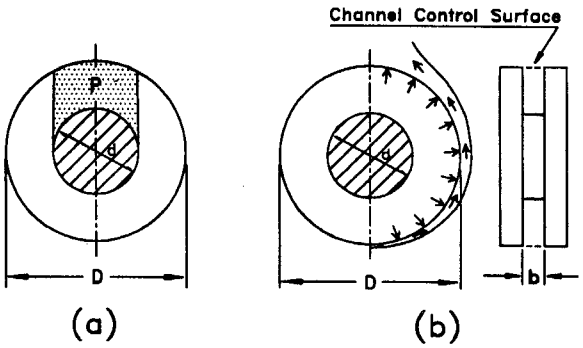

Fig. 3(*a*) Area affected by cylinder plume; (*b*) external heat transfer of narrow channel

$$\mathrm{Nu} = \mathrm{Nu}^0 + F(\mathrm{Pr})G_{\sqrt{A}}(D/\sqrt{A})^{1/4}\mathrm{Ra}^{1/4}. \quad (8)$$

Equation (8) will be used in the following modeling for air cooling, with Pr = 0.71 and $F(\mathrm{Pr}) = 0.513$.

Diffusive Limit. The diffusive limit of the circumscribed cylinder of the heat sink is taken to represent the heat sink. Based on b and A_{HS}, the contribution by the diffusive limit to the total heat transfer of the heat sink can be calculated using (Yovanovich 1987a)

$$\mathrm{Nu}^0 = \left\{\frac{3.1915 + 2.7726\,(L/D)^{0.76}}{\sqrt{1 + 2(L/D)}}\right\}\frac{\sqrt{A_{CC}\cdot b}}{A_{HS}}. \quad (9)$$

Nusselt Number for Outer Surface. It is assumed that the boundary layer flows over the fin rims do not interact with the boundary layer flows associated with the lateral and end surfaces. Because the body-gravity function is insensitive to changes in geometry and orientation of bodies (Lee et al., 1991), the above assumption will not introduce much deviation in the total body-gravity function of the heat sink.

The body-gravity functions of a fin rim and an end surface can be calculated separately using Eq. (5) as $0.891(t/D)^{1/8}$ and 1.021, respectively. The overall body-gravity function for the outer surface, $G_{\sqrt{A_{\mathrm{OUT}}}}$, can be obtained using Eq. (6) as

$$G_{\sqrt{A_{\mathrm{OUT}}}} = (0.891\,tN_fD^{3/4} + 0.607D^{7/4})\left(\frac{\pi}{A_{\mathrm{OUT}}}\right)^{7/8}. \quad (10)$$

The boundary layer heat transfer from the outer surface can be calculated using the second term of Eq. (8). Based on the heat sink surface area A_{HS}, the contribution of the outer surface to the total heat transfer is

$$\mathrm{Nu}_{\mathrm{OUT}} = \left\{0.513\,G_{\sqrt{A_{\mathrm{OUT}}}}\left(\frac{D}{\sqrt{A_{\mathrm{OUT}}}}\right)^{1/4}\mathrm{Ra}^{1/4}\right\}\frac{A_{\mathrm{OUT}}}{A_{HS}} \quad (11)$$

Nusselt Number for Inner Surface.

Boundary Layer Solution for Inner Surface. For $\mathrm{Ra} > 10^3$, the boundary layers formed over adjacent fins do not interact, and, hence, the average heat transfer over the inner surface will be close to that of external convection with the same surface area. In these circumstances, the external natural convection solutions can be directly applied to the inner surface.

For the support cylinder surface between two adjacent fins, the body-gravity function is $0.891(b/d)^{1/8}$. In order to take into account the effect of the plume rising from the support cylinder upon the lateral fin surface heat transfer, as shown in Fig. 3(*a*), the heat transfer rate from area P will be reduced by half based on the fact that the temperature difference between the area P and the plume is approximately $(T_S - T_\infty)/2$. The body-gravity function of a fin lateral surface, with the effect of the plume, can be obtained by $1.021 - 0.317(d/D) + 0.302(d/D)^2$. The body-gravity functions of the inner surface components are combined using Eq. (6) to give the body-gravity function for the inner surface, $G_{\sqrt{A_{\mathrm{IN}}}}$.

$$G_{\sqrt{A_{\mathrm{IN}}}} = (N_f - 1)\left(\frac{\pi}{A_{\mathrm{IN}}}\right)^{7/8}\{0.891\,bd^{3/4} + [0.607 - 0.188\,(d/D) + 0.18\,(d/D)^2](D^2 - d^2)^{7/8}\}. \quad (12)$$

The boundary layer Nusselt number for the inner surface can be obtained using the second term of Eq. (8):

$$\mathrm{Nu}_{bl} = 0.513\,G_{\sqrt{A_{\mathrm{IN}}}}(D/\sqrt{A_{\mathrm{IN}}})^{1/4}\mathrm{Ra}^{1/4}. \quad (13)$$

Fully Developed Flow Solution for Inner Surface. Two adjacent fins of the heat sink form a channel. In the fully developed regime, the heat transferred from the channel surface consists of the following two parts: (1) the heat carried away by the channel flow; and (2) the heat conducted radially outward from the channel.

1 From the analysis of fully developed flow (Elenbaas, 1942), the Nusselt number for the channel flow based on one channel surface area can be approximated by (Wang, 1997)

$$\mathrm{Nu}_{cf} = \frac{1}{12}\mathrm{Ra}\,\frac{D\sqrt{D^2 - d^2}}{A_{CL}}. \quad (14)$$

2 When Ra is very small, e.g., as the spacing b becomes small, the channel flow will be restricted, and the rate of heat flow carried away by the channel flow will be minimal. Under these circumstances heat will be transferred out of the channel primarily by conduction, and then result in convection outside the channel, as shown in Fig. 3(*b*). This portion of the heat transfer will be approximately modeled as convective heat transfer from an isothermal, cylindrical surface with diameter D and width b. This imaginary surface is referred to as a channel control surface as shown in Fig. 3(*b*) and its body-gravity function, $G_{\sqrt{A_{\mathrm{cs}}}}$, is $0.891(b/D)^{1/8}$.

The heat transfer at this surface can also be calculated using the second term of Eq. (8) and then converted to be based on the channel surface area A_{CL}.

$$\mathrm{Nu}_{cs} = \left\{0.513\,G_{\sqrt{A_{\mathrm{cs}}}}\left(\frac{D}{\sqrt{A_{CS}}}\right)^{1/4}\mathrm{Ra}^{1/4}\right\}\frac{A_{CS}}{A_{CL}}. \quad (15)$$

The heat transfer from the inner surface in the fully developed regime can be found by

$$\mathrm{Nu}_{fd} = \mathrm{Nu}_{cf} + \mathrm{Nu}_{cs}. \quad (16)$$

Blending Two Limiting Solutions. The composite solution technique suggested by Churchill and Usagi (1972) is used to combine the two limiting solutions to give the inner surface Nusselt number for a full range of Ra. Based on A_{HS}, the inner surface contribution to the total heat transfer is

$$\mathrm{Nu}_{\mathrm{IN}} = \frac{A_{\mathrm{IN}}/A_{HS}}{[(1/\mathrm{Nu}_{bl})^n + (1/\mathrm{Nu}_{fd})^n]^{1/n}}. \quad (17)$$

The concept of combining the two limits to give the channel solution first appeared in the work of Churchill (1977). Based on the comparisons with the present experimental data and the previous correlations, $n = 1$ was chosen for heat sink applications.

This value of n is different from the previous values of n for parallel plates, such as $n = 1.5$ (Churchill, 1977), $n = 2$ (Kraus and Bar-Cohen, 1983), $n = 1.9$ (Raithby and Hollands, 1985), because the interference of the support cylinders changes the behavior of the channel heat transfer. Actually if different values of n are used for different diameter ratios of D/d, the model will give better predictions for each case of D/d. But for the

Table 1 Functions of simplified model

Functions	Parameter Ranges
$f_1 = [3.36 + 0.087(L/D)]\sqrt{A_{CC}\cdot b/A_{HS}}$	$L/D < 10$
$f_2 = [0.449 - 0.026\ln(t\,N_f/D)]A_{OUT}/A_{HS}$	$0.01 < t\,N_f/D < 10$
$f_3 = 0.573 - 0.184(d/D) + 0.0388(d/D)^2$	$6.3 \times 10^3 < Ra_D < 1.2 \times 10^6$ and $0.1 \le d/D \le 0.8$
$f_4 = 0.0516 + 0.0154(d/D) - 0.0433(d/D)^2 + 0.0792(d/D)^3$	
$f_5 = 0.0323 - 0.0517(d/D) + 0.11(d/D)^2$	

purpose of simplicity, $n = 1$ was chosen for heat sink applications. In practice the diameter ratio D/d of the heat sinks does not change very much, usually ranging from 1.6 to 3.6 for the heat sinks used in electronic systems.

Nusselt Number for Heat Sink. The total heat transfer from the heat sink can be found by combining the three contributions, namely, the heat transfer from the inner surface, the boundary layer heat transfer from the outer surface, and the diffusive limit. Therefore, the model for the heat sink is obtained as

$$\mathrm{Nu} = \mathrm{Nu}^0 + \mathrm{Nu}_{\mathrm{OUT}} + \mathrm{Nu}_{\mathrm{IN}} \tag{18}$$

Simplified Model. In order to make the calculation of Nu in Eq. (18) easier, the following correlation equations were obtained through fitting the predictions of Eq. (9), Eq. (11), and Eqs. (13–15):

$$\mathrm{Nu}^0 = f_1 \tag{19}$$

$$\mathrm{Nu}_{\mathrm{OUT}} = f_2 \mathrm{Ra}^{1/4} \tag{20}$$

$$\mathrm{Nu}_{\mathrm{IN}} = \frac{A_{\mathrm{IN}}/A_{HS}}{1/\mathrm{Nu}_{bl} + 1/\mathrm{Nu}_{fd}}, \tag{21}$$

where

$$\mathrm{Nu}_{bl} = f_3\,\mathrm{Ra}^{1/4} \tag{22}$$

$$\mathrm{Nu}_{fd} = f_4\,\mathrm{Ra} + f_5\,\mathrm{Ra}^{1/4}. \tag{23}$$

The functions f_1, f_2, f_3, f_4, f_5 and their parameter ranges are given in Table 1. For the range of Ra from 10 to 10^4, the maximum difference between the predictions by the model and its simplified equations is within 5 percent and the RMS difference is within 3 percent. Although the model was simplified for heat sinks within the parameter ranges, it may also be used outside the ranges.

Trends of Model Predictions

The model predictions for the heat sinks used in this study are shown in Fig. 6 for a wide range of Ra between 10^{-2} and 10^5. They are the five fine curves A, B, C, D, and E. The geometric dimensions of the five heat sinks are given in Table 2. In these plots, geometric parameters are fixed for each curve, Ra varies with Ra_D (note: $\mathrm{Ra} = \mathrm{Ra}_D \cdot b^4/D^4$). The top dashed line represents a solid horizontal circular cylinder, (specifically,

Table 2 Geometric parameters of test heat sinks (d = 22, D/d = 1.66, length unit: mm)

Heat Sink	b	t	N_f	L	D	A_{HS}
A	22.5	10	3	75	36.5	11308
B	7.5	9	5	75	36.5	14656
C	4	9	6	74	36.5	16329
D	2	9	7	75	36.5	18141
E	1	10	7	76	36.5	18529

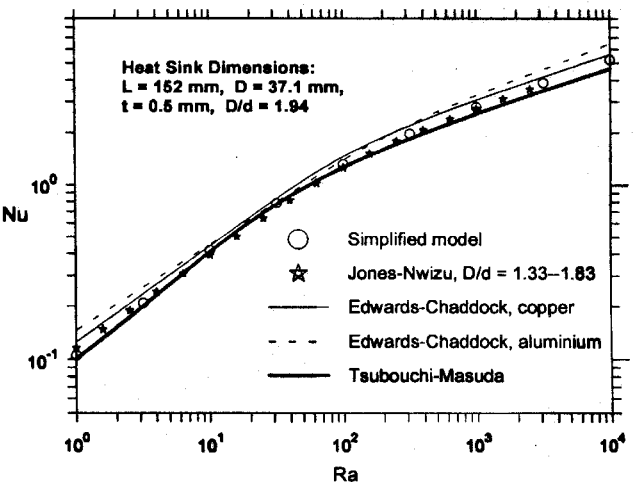

Fig. 4 Comparisons of simplified model with previous correlations (D/d = 1.94)

L = 75 mm, D = 36.5 mm, d/D = 0.999, t = 20 mm, b = 35 mm, and N_f = 2). The bottom thick solid curve represents a heat sink with the same d/D as the test heat sinks but with very small fin thickness and a large number of fins. In this case, the area ratio A_{OUT}/A_{HS} is very small, the inner surface heat transfer is dominant in the entire range of Ra, so the curve is similar to a channel heat transfer curve. For the heat sinks, when b/D is large, there are fewer fins and the area ratio A_{OUT}/A_{HS} is relatively large, the channeling effect will be small and the heat transfer curve will be similar to a solid cylinder curve, i.e., curve A in Fig. 6. When b/D is small, especially with a small fin thickness t and a large number of fins, N_f, the area ratio A_{OUT}/A_{HS} is small, the channeling effect will be large and the heat transfer curve will be close to the channel curve.

If L/D, t/D, and d/D of the heat sink and Pr are fixed, as is common practice by most researchers, Nu is a function of two parameters, i.e., $\mathrm{Nu} = f(\mathrm{Ra}, b/D)$, as shown in Fig. 6, where for each value of Ra there are multiple values of Nu corresponding to different heat sinks or different b/D. Similar trends of numerical results for parallel plate channels were reported previously by Martin et al. (1991) and Li and Chung (1996). Therefore, comparisons with previous experimental data should be made in such a way that at each Ra value, the present value of b/D is the same as that in the previous experiments, especially at low Ra. And the end surfaces and the fin thickness should also be taken into consideration.

Comparisons to Previous Correlations and Present Experimental Data

In the previous experiments (Edwards and Chaddock, 1963; Jones and Nwizu, 1969; Tsubouchi and Masuda, 1970), Ra_D was more or less fixed and the wide range of Ra was achieved by variation of b/D (note: $\mathrm{Ra} = \mathrm{Ra}_D \cdot b^4/D^4$). Therefore, in the following comparisons, the present model predictions are given in such a way that Ra_D is fixed at an average value and Ra varies with b/D. In addition, the heat sink dimensions used by Edwards and Chaddock (1963) are adopted for the present model. In their experiments, the length of the heat sinks, L, the thickness of fins, t, and the diameter of support cylinder, d, were fixed. They made measurements for three cases of the diameter ratio (D/d = 1.94, 2.97, and 5.17).

In the previous experiments, the radiation losses were calculated and subtracted from the total heat flow rate.

In Fig. 4, the simplified model is compared with the previous correlations for D/d = 1.94. The maximum difference between the model and the Jones-Nwizu correlation is 9.8 percent and

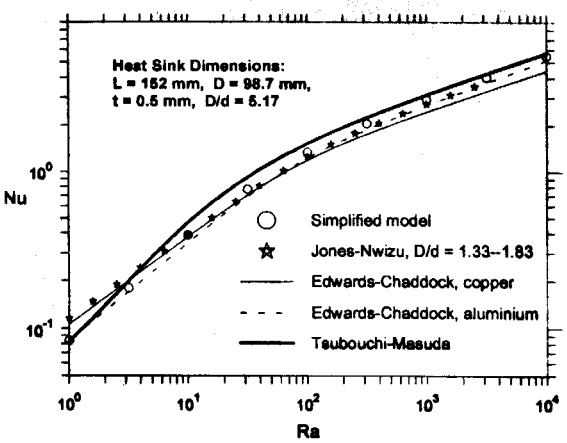

Fig. 5 Comparisons of simplified model with previous correlations (D/d = 5.17)

the RMS difference is 5.4 percent. While the maximum and the RMS differences between the model and the Tsubouchi-Masuda correlation are 11.3 percent and 6.4 percent, respectively.

The comparisons for D/d = 5.17 are shown in Fig. 5. Between the model and the Edwards–Chaddock correlation for aluminum fins, the maximum and RMS differences are 11.5 percent and 8.1 percent, respectively. From Ra = 10 to 10^4, the maximum difference between the model and the Jones–Nwizu correlation is 7.1 percent and the RMS difference is 6.2 percent.

The present model takes into account the end surface heat transfer, while the Jones–Nwizu and the Tsubouchi–Masuda correlations do not. Because the number of fins is quite large in the above comparisons (N_f = 80 for Ra = 1), the end surface effect becomes negligible.

Five heat sinks were tested in the present experiments. Their geometric dimensions are given in Table 2, where N_f is the number of fins and A_{HS} is the total surface area of the heat sink. A cartridge heater was embedded in the center of the heat sink to provide a source for internal heat generation. The heat sink was suspended horizontally, as shown in Fig. 1, in the center of a large enclosure with quiescent air as the cooling fluid. All surfaces, including the two end surfaces, were exposed to the cooling fluid. The experiments were carried out at atmospheric pressure, and the temperature differences between the heat sink and the ambient air ranged from 20 K to 80 K. Six to eight thermocouples were embedded under the surface of the heat sink at various locations to provide a true measure of the heat sink temperature. Care was taken to prevent the thermocouple wire heat transfer from disturbing the temperature fields around the thermocouples. The maximum temperature difference between any two thermocouples was 0.25 K when $T_S - T_\infty$ = 50 K, so the heat sink surface was considered as isothermal.

The radiation losses were measured in a vacuum chamber for each heat sink at different temperature levels. In data reduction, these amounts of radiation losses were subtracted from the total heat transfer rate measured in convection experiment. The heat losses through the power leads and the thermocouple wires were also accounted for in the data reduction. The uncertainty analysis (Wang, 1997) showed that the uncertainty in Ra was within ±5.1 percent and the uncertainty in Nu was within ±2.0 percent.

The experimental results are compared with the simplified model in Fig. 6 along with three other correlations, where the dimensions of the test heat sinks are used in the model. In this comparison Ra varies with Ra_D. Although the five heat sinks were tested at the similar conditions, i.e., the Ra_D are close to one another, the experimental results (square symbols) lie in different ranges of Ra because they have different values of b/D. In the order A, B, C, D, and E, the experimental results of the heat sinks lie in the range of Ra = 2×10^4 to 10^{-1}. The curves A, B, C, D, and E represent the model predictions for the five heat sinks. The agreement between the experimental data and the model is very good. The maximum and RMS percentage differences between the model and the data for each of the five heat sinks are A(7.5, 5.1), B(6.4, 5.6), C(4.2, 2.8), D(3.3, 2.5), and E(3.5, 2.5), respectively.

In the range of Ra > 4×10^3 the boundary layer heat transfer is dominant, so the experimental results of heat sink A lie along a straight line of slope $\frac{1}{4}$. For Ra = 10^3 to 10^0, the introduction of channeling effects results in increases in the slopes of the curves. For Ra < 10^{-1}, the boundary layer heat transfer from the outer surface of heat sink E becomes dominant, and the slope of curve E returns to $\frac{1}{4}$. Figure 6 also shows that the previous correlations can not predict heat transfer from these heat sinks at low Ra. Since there are just a few fins on these heat sinks, the end surfaces play a significant role in the total heat transfer, and the heat transfer from the fin rim surfaces is significant in these cases due to the large fin thickness. These two factors were not considered in the previous correlations, therefore they cannot account for the heat transfer from the end surfaces and the larger fin rim surfaces, and, hence, give lower predictions for the test heat sinks at low Ra.

Application Related Issues

Radiative Dissipation. In the natural convection regime, radiation can play an important role in electronic cooling. A set of equations for calculating radiative losses from annular heat sinks was given by Wang et al. (1997) and Wang (1997).

Mounted Heat Sinks. Annular-fin heat sinks used in electronic applications are usually mounted by bonding one end of the heat sink to a flat surface of a component, while the other end is exposed to the cooling fluid. Therefore, only one end of the heat sink acts as an active surface for natural convection cooling. Because the proposed method is flexible, the boundary condition on each of the end surfaces can be specified independently, allowing this configuration to be modeled.

Nonisothermal Surface. Heat sinks used in practical applications are not truly isothermal, although in many cases the temperature variation on the heat sink surface is small. To account for this temperature variation, an average temperature of the heat sink surface may need to be found before using the model for the heat sinks. This can be done through a fin efficiency analysis. The average temperature can be taken as the isothermal temperature of the heat sink in the model. Hahne and Zhu (1994) made comparisons between two sets of results,

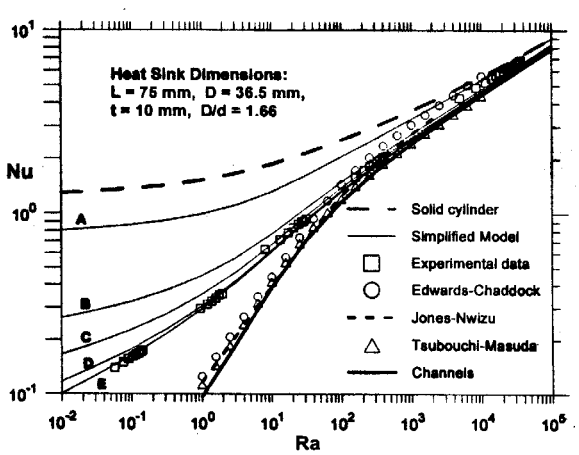

Fig. 6 Comparison of simplified model with present experimental data

one was obtained using the total surface area and the average temperature, the other was calculated with subsurface areas and their local temperatures. They found that the difference between the two sets of data was less than 1 percent. This supports the approach stated above. In cases with small surface temperature variations, finding the average surface temperature may not be necessary and the isothermal assumption will provide accurate results.

Summary and Conclusions

The boundary layer solution for laminar natural convection, the fully developed flow solution and the diffusive limit are successfully applied to the isothermal vertical disks with horizontal support cylinders. A general model for laminar natural convection heat transfer from this geometry has been developed and applied to annular heat sinks. The model accounts for the effects of the end surfaces and the fin thickness, and overcomes the shortcomings of the previous correlations.

A simplified model is presented and compared with previous correlations and new experimental data. Very good agreement can be seen in these comparisons. The previous correlations fail to predict the present experimental data at the fully developed regime, because they do not take into consideration the effects of the end surfaces and the fin thickness.

Acknowledgments

The authors acknowledge the financial support of the Natural Sciences and Engineering Research Council of Canada and The Manufacturing Research Corporation of Ontario. The authors also acknowledge Pete Teertstra for his help with the final revision of this paper.

References

Acrivos, A., 1960, "A Theoretical Analysis of Laminar Natural Convection Heat Transfer to Non-Newtonian Fluids," *AIChE Journal,* Vol. 6, No. 4, pp. 584–590.

Churchill, S. W., and Usagi, R., 1972, "A General Expression for the Correlation of Rates of Transfer and Other Phenomena," *AIChE Journal,* Vol. 18, pp. 1121–1128.

Churchill, S. W., and Churchill, R. U., 1975, "A Comprehensive Correlating Equation for Heat and Component Transfer by Free Convection," *AIChE Journal,* Vol. 21, pp. 604–606.

Churchill, S. W., 1977, "A Comprehensive Correlating Equation for Buoyancy-Induced Flow in Channels," *Letters in Heat and Mass Transfer,* Vol. 4, pp. 193–199.

Edwards, J. A., and Chaddock, J. B., 1963 "An Experimental Investigation of the Radiation and Free-Convection Heat Transfer from a Cylindrical Disk Extended Surfaces," *Trans. ASHRAE,* Vol. 69, pp. 313–312.

Elenbaas, W., 1942, "Heat Dissipation of Parallel Plates by Free Convection," *Physica,* Vol. IX, No. 1, pp. 1–28.

Hahne, E., and Zhu, D., 1994, "Natural Convection Heat Transfer on Finned Tubes in Air," *Int. J. Heat Mass Transfer,* Vol. 37, Suppl. 1, pp. 59–63.

Jones, C. D., and Nwizu, E. I., 1969, "Optimum Spacing of Circular Fins on Horizontal Tubes for Natural Convection Heat Transfer," *ASHRAE Symp.,* Bull. DV-69-3, pp. 11–15.

Kraus, A. D., and Bar-Cohen, A., 1983, "Thermal Analysis and Control of Electronic Equipment," Hemisphere Publishing Corporation, New York.

Lee, S., Yovanovich, M. M., and Jafarpur, K., 1991, "Effects of Geometry and Orientation on Laminar Natural Convection from Isothermal Bodies," *J. Thermophysics and Heat Transfer,* Vol. 5, No. 2, pp. 208–216.

Li, H.H., and Chung, B. T. F., 1996, "A New Look at Natural Convection from Isothermal, Vertical Parallel Plates," HTD-Vol. 333, Proceedings, ASME Heat Transfer Division, Vol. 2, ASME, New York, pp. 249–256.

Martin, L., Raithby, G. D., and Yovanovich, M. M., 1991, "On the Low Rayleigh Number Asymptote for Natural Convection Through an Isothermal, Parallel-Plate Channel," ASME *Journal of Heat Transfer,* Vol. 113, pp. 899–905.

Raithby, G. D., and Hollands, K. G. T., 1975, "A General Method of Obtaining Approximate Solutions to Laminar and Turbulent Free Convection Problems," *Advances in Heat Transfer,* T. F. Irvine, Jr., and J. P. Hartnett, eds., Vol. 11, Academic Press, New York, pp. 264–315.

Raithby, G. D., and Hollands, K. G. T., 1978, "Analysis of Heat Transfer by Natural Convection (or Film Condensation) for Three Dimensional Flows," Proceedings, 6th International Heat Transfer Conf., Toronto, August 7–11, Vol. 2, pp. 187–192.

Stewart, W. E., 1971, "Asymptotic Calculation of Free Convection in Laminar Three-Dimensional Systems," *Int. J. Heat Mass Transfer,* Vol. 14, pp. 1013–1031.

Tsubouchi, T., and Masuda, H., 1970, "Natural Convection Heat Transfer from Horizontal Cylinders With Circular Fins," Proceedings, 4th Int. Heat Transfer Conf., Paper NC 1.10, pp. 1–11.

Wang, C.-S., Yovanovich, M. M., and Culham, J. R., 1997, "General Model for Natural Convection: Application to Annular-Fin Heat Sinks," HTD-Vol. 343, Proceedings, 32nd National Heat Transfer Conference, Vol. 5, ASME, New York, pp. 119–128.

Wang, C.-S., 1997, "Laminar Natural Convection Heat Transfer from Isothermal Horizontal Cylinders with Annular Fins," Ph.D. thesis, Department of Mechanical Engineering, University of Waterloo, Waterloo, Canada.

Yovanovich, M. M., 1987a, "New Nusselt and Sherwood Numbers for Arbitrary Isopotential Geometries at Zero Peclet and Rayleigh Numbers," AIAA Paper No. 87-1643.

Yovanovich, M. M., 1987b, "Natural Convection from Isothermal Spheroids in the Conductive to Laminar Flow Regimes," AIAA Paper no. 87-1587.

Yovanovich, M. M., 1987c, "On the Effect of Shape, Aspect Ratio and Orientation Upon Natural Convection from Isothermal Bodies of Complex Shapes," paper presented at the 1987 ASME National Heat Transfer Conference.